LAIKIPIA UNIVERSITY JOURNAL OF SCIENCE AND APPLIED TECHNOLOGY

Studies on a Fabricated Novel Carbon Nanotube-Infused Polysulfone Nanocomposites

Shisia K. Silvanus
Department of Chemistry and Biochemistry,
Laikipia University,
P.O Box 1100, Nyahururu, Kenya

Corresponding email: sshisia@laikipia.ac.ke

Abstract

Water pollutants such as heavy metals and polycyclic aromatic hydrocarbons have adverse effects on humans and environment. Prolonged exposure to low concentrations of these pollutants over time may lead to disposition of ailments which are health hazards. Conventional water treatment methods such as flocculation, sedimentation, and filtration do not remove dissolved trace levels of such pollutants. This work aimed at investigating the potential of fabricated model of magneto-responsive Carbon nanotube (CNT)-polysulfone (PSF) infused polymeric nanocomposites in water purification against oil spills and heavy metals pollution. The CNTs were prepared by thermal catalysed vapour deposition (TCVD) while magnetite nanoparticles were prepared by solvothermal and stober processes. The CNTs were decorated with PSF polymer before infusion of the core shell Fe_3O_4-SiO_2. The fabricated nanocomposites were applied in removal of trace pollutants through adsorption process. Regeneration tests were performed on both the nanocomposites as well as to the existing carbon-based adsorbents to ascertain workability of the product. The nanocomposite was characterized for structure and morphology using scanning electron microscopy (SEM), Transmission electron microscopy (TEM), Fourier Transform infra-red (FT-IR), Energy Dispersive spectroscopy (EDS) and X-ray diffraction (XRD) while its magneto-responsiveness was tested by Superconducting quantm interference Device (SQUID). The presence of absorption band in IR spectrum at 460 cm^{-1} and 521 cm^{-1} was for the vibrations of Fe-O bond in Fe_3O_4 nanoparticles formed. The core shell nanoparticles obtained displayed a thin hysteresis loop having saturation magnetization 2.2 emu g^{-1} with ferromagnetic property. Adsorption of Pb(II) ions followed pseudo second-order while Freundlich adsorption isotherm gave the best-fit for the two pollutants.

Keywords: characterization, fabrication, nanocomposites, regeneration, water pollutants, treatment methods

Introduction

Different polymer nanocomposites have been used in removing heavy metal ions from the aqueous solution typically in the treatment of contaminated water. Carbon nanotubes (CNTs) have proved as better adsorbents than activated carbon for removal of many heavy metals. Nanomaterials with distinct external functionalization features are desirable in fabrication due to enhanced surface properties that lead to excellent adsorptions. Attachment of functional groups onto the nanomaterials as shown in figure 1 induces unique characteristics such as high selectivity and rapid desorption to the adsorbents.

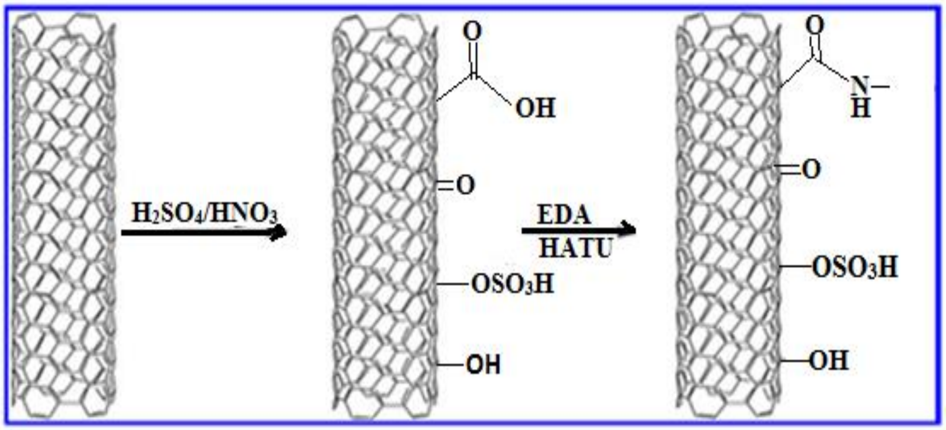

Fig. 1. CNTs functionalization process (Díez-Pascual, 2021)

The nature of nanoparticles largely depend on their independent compositions and dependent surface structures (Sun et al., 2012). The physical and chemical properties of nanoparticles usually deviate from those in their bulk form due to a decrease in their particle sizes. Dispersion of CNTs in a polymer solution could be very difficult to achieve due to the strong van der Waals interactions between them (Han and Fina, 2011). However, the homogenous dispersion can be realized by various CNTs functionalization schemes. Covalent functionalization of CNTs by strong acids inevitably generates defects on the walls of CNTs which degrades its electrical properties (Banerjee et al; 2005). Non-covalent functionalization of CNTs using polysulfone polymer overcomes such limitations. Polysulfones (PSF) are members of thermoplastic polymers known for their toughness and stability at high temperatures. Polysulfone molecules are planar conjugates with sp^2 hybridized structures and they can disperse CNTs easily through π-π interactions.

(Mallick, 2007). Incorporation of inorganic nanoparticles into polymeric system can enhance mechanical and thermal stability of polymeric membranes (Yin and Deng, 2015).

Materials and Methods

This study involved fabrication and characterization of CNT-IPSF/Fe_3O_4 nanocomposites from synthesized carbon nanotubes (CNTs), magnetite NPs and core shell NPs (Figure 2).

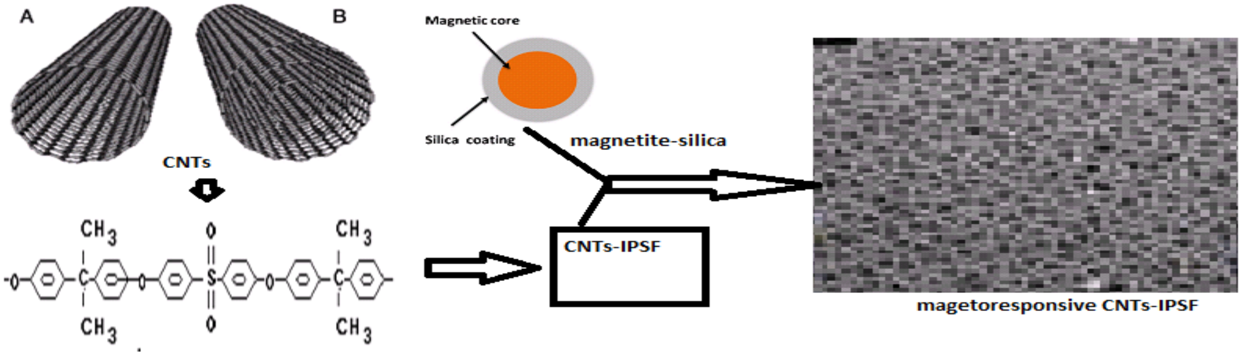

Fig. 2. Fabrication Process

This was followed by determining efficiency of fabricated CNT-IPSF/Fe_3O_4 nanocomposites in removal of lead ions from polluted water samples. These efficiencies were compared to those on commercial activated carbon. Adsorption and desorption studies on the CNT-IPSF/Fe_3O_4 nanocomposites were carried out to test the nanocomposite for its reusability.

Results and Discussion

The prepared CNTs were characterization for morphology by scanning electron microscopy (SEM) and shown as images in Figure 3(a). This SEM image depicts configuration of the prepared material as abundant threadlike entities. The SEM images further provided evidence that the twisting and winding entities are for CNTs which was confirmed by transmission electron microscopy (TEM) as in Figure 3(b).

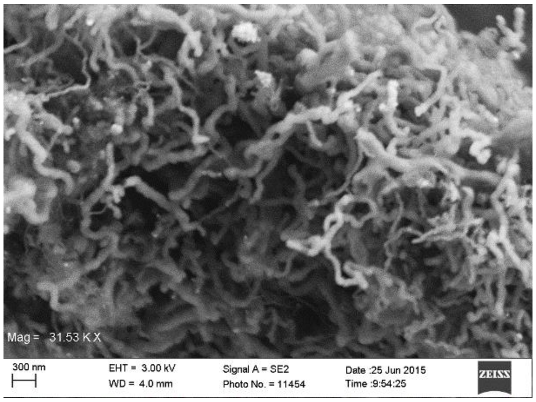

Fig. 3 (a) SEM for CNTs

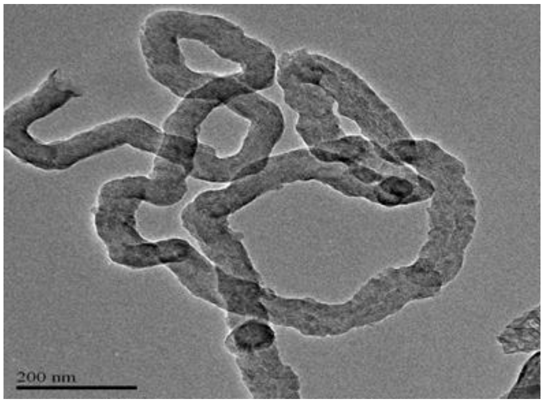

Fig. 3 (b) TEM for CNTs

The magnetite core (Fe_3O_4) and core shell ($Fe_3O_4.SiO_2$) nanoparticles were characterized as shown by the SEM micrographs in figure 4(a) and figure 4(b) respectively. It can be observed that large quantities of aggregated magnetite nanoparticles are formed with moderately uniform and oval shapes.

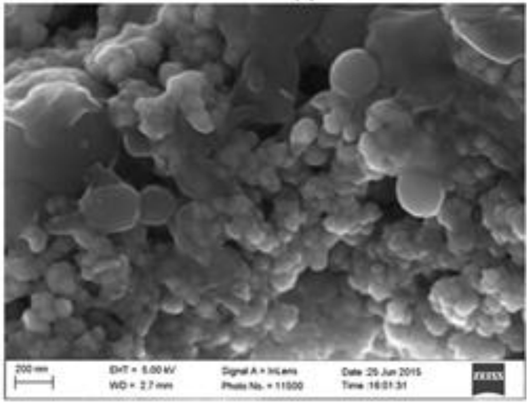

Fig. 4 (a) SEM for core Fe_3O_4

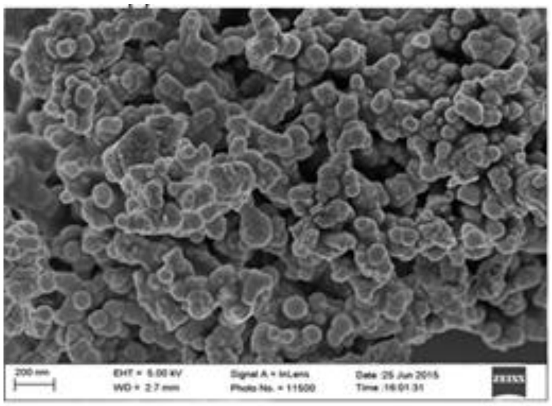

Fig. 4 (b) SEM for core shell $Fe_3O_4.SiO_2$) Nps

The SEM analysis was done to determine surface distribution of synthesized nanoparticles. The SEM images for the core shell ($Fe_3O_4.SiO_2$) nanoparticles depicts an arrangement of a closed packed manner, with varying pores for the synthesized nanoparticles. This property of the nanoparticles is suitable for many applications involving its incorporation during nanocomposites fabrication (Wei et al., 2012; Sodipo & Aziz, 2013). The X-ray diffraction pattern (figure 5) of the core shell NPs matched the same pattern for the magnetite (Fe_3O_4) phase as compared to standard XRD patterns reported elsewhere.

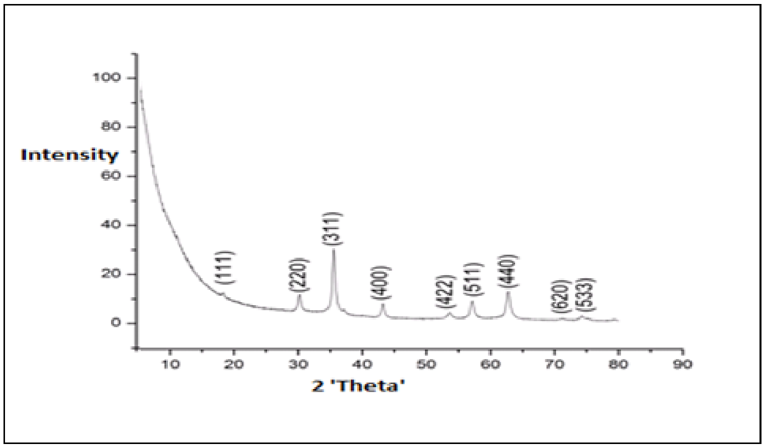

Fig. 5.XRD pattern for Core Shell NPs

The peaks at (220), (311), (400), (422), (511) and (440) planes correspond to a cubic unit cell, for a cubic spinel structure due to the strongest reflection that proceeds from the (311) plane. The peak width broadening is most pronounced at greater angles 2θ. Further, the instrumental profile width broadening is also largest at large angles 2θ. However, peak intensity is usually weakest at larger 2θ angles. Therefore, the use of a single more intense peak, often gives better results from diffraction peaks between 30 and 50 deg 2θ. From figure 5, the most intense peak appearing at 35.52 deg 2θ was used in determination of crystalline sizes. Peak width of the crystallites varies inversely with crystallite size, for instance, as the peak gets broader, the crystallite size gets smaller (Rehani et al; 2006).

Fitting the XRD data to Gaussian (figure 6 a) and Lorentz line profile (figure 6b), two patterns were obtained from which crystallite size was determined. Crystallite size measurements were determined as 22.4 nm from the strongest reflection of the (311) peak. This was based on the Debye-Scherrer approximation, which assumes that small sizes of crystallites cause line broadening (Shaaban et al; 2013). The diffraction pattern showed that the synthesized core shell nanoparticles were crystalline, while the position and the relative intensity of the diffraction peaks matched the standard XRD data from JCPDS file No. 19-0629 (Zhan et al., 2011).

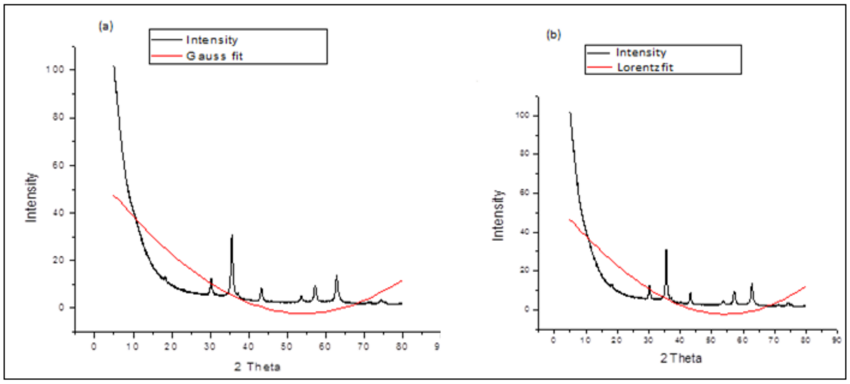

Fig. 6. Line profiles for (a) Gaussian and (b) Lorentz for magnetite silica NPs

Fourier transform infrared spectroscopy was used to analyse the surface of the magnetite core before and after functionalization with silica to form core shell nanoparticles (Figure 7).

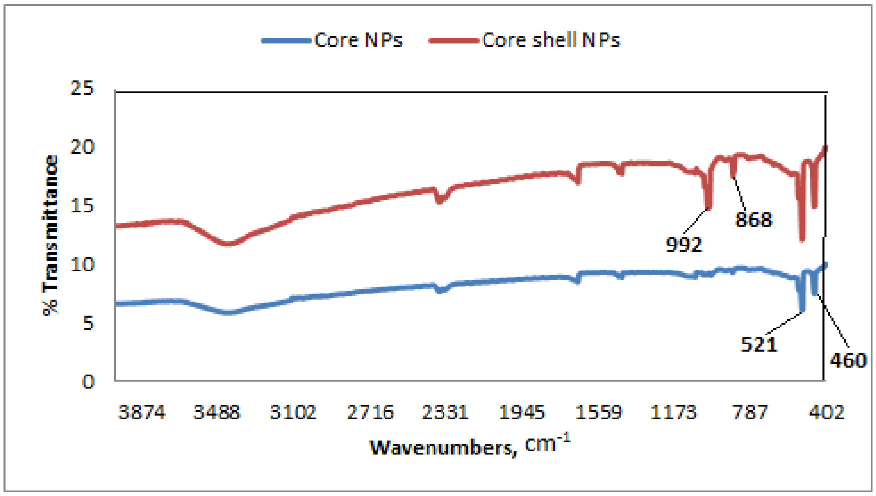

Fig. 7. IR spectra for magnetite core and core shell nanoparticles

The presence of absorption band between 460 cm^{-1} and 521 cm^{-1} is assigned to the vibrations of Fe−O bonding in magnetite core (Fe_3O_4) nanoparticles Yang et al; 2008). The absorption band at 521 cm$^{−1}$ could also be due to the Fe–O bonds in tetrahedral positions of the spinel inverse structure of the magnetite nanoparticles. In the spectrum of the core shell nanoparticles, additional bands were found at 992 cm$^{−1}$ and 868 cm$^{−1}$ which confirmed stretching−vibration bands for Si–O and

Si–O–Si bonds respectively. The Si−O and Si–O–Si stretching vibration bands confirmed the formation of SiO_2 shell on Fe_3O_4 core nanoparticles (Kulkarni et al., 2014).

The adsorption of selected cations (Pb^{2+}, Zn^{2+}, Cu^{2+} and Cd^{2+}) by CNT-IPSF/Fe_3O_4 nanocomposites and activated carbon adsorbents was also studied (Figure 8).

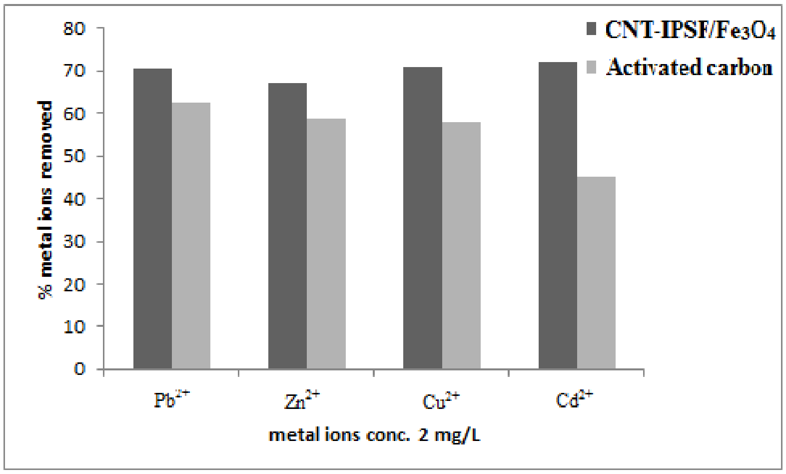

Fig. 8 Cations adsorption onto CNT-IPSF/Fe_3O_4 and activated carbon

It can be seen that the CNT-IPSF/Fe_3O_4 nanocomposites had higher removal efficiency (≥70 %) for all cations studied than activated carbon adsorbent ($p=0.005$). This confirmed that the CNT-IPSF/Fe_3O_4 nanocomposite can be used to remove cationic pollutants from aqueous solutions.

The Freundlich and Langmuir isotherm were derived from the equilibrium data. Accordingly, the R^2 values were above 0.99 (table 1) implying that the Freundlich model fitted the experimental data better than Langmuir model (Ismail et al., 2013).

Table 1. Langmuir and Freundlich adsorption isotherm constant for Pb(II) ions on CNT-IPSF/Fe_3O_4 and activated carbon adsorbents

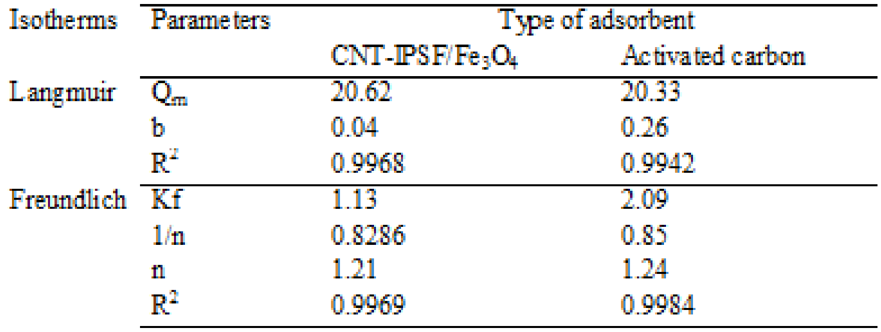

Isotherms	Parameters	Type of adsorbent	
		CNT-IPSF/Fe_3O_4	Activated carbon
Langmuir	Q_m	20.62	20.33
	b	0.04	0.26
	R^2	0.9968	0.9942
Freundlich	Kf	1.13	2.09
	1/n	0.8286	0.85
	n	1.21	1.24
	R^2	0.9969	0.9984

The fact that the correlation coefficient, i.e., $R^2 > 0.99$ for both CNT-IPSF/Fe_3O_4 and activated carbon suggests that both isotherms provide a good result for the adsorption model of Pb(II) ions. From the Freundlich isotherm model, the Pb(II) ions adsorbed for a unit equilibrium concentration (K_f) were 1.13 and 2.09 for CNT-IPSF/Fe_3O_4 nanocomposites and activated carbon adsorbents respectively. The K_f value is related to the adsorption intensity. Therefore, the K_f values from this study ($1 < K_f$) confirmed that the adsorption capacity was high. The adsorption intensity value for CNT-IPSF/Fe_3O_4 nanocomposites of n=1.21 was $1< n < 10$ representing beneficial adsorption of Pb (II) ions (Zheng et al., 2009).

The desorption of Pb(II) ions from the CNT-IPSF/Fe_3O_4 nanocomposites was investigated using selected solvents, i.e., de-ionized water, 0.1M HNO_3 and 0.1M EDTA so as to identify the most suitable desorption solvent for removal of the adsorbed Pb(II) ions from the nanocomposites. The efficiency of selected desorption solvents in removal of the adsorbed Pb(II) ions from the surfaces of the CNT-IPSF/Fe_3O_4 nanocomposites and standard activated carbon adsorbents showed that 0.1M EDTA was favoured (Figure 9). This desorption test, if reliable, could positively impact the subsequent utilization of the nanocomposites, thus providing higher chances for its reusability.

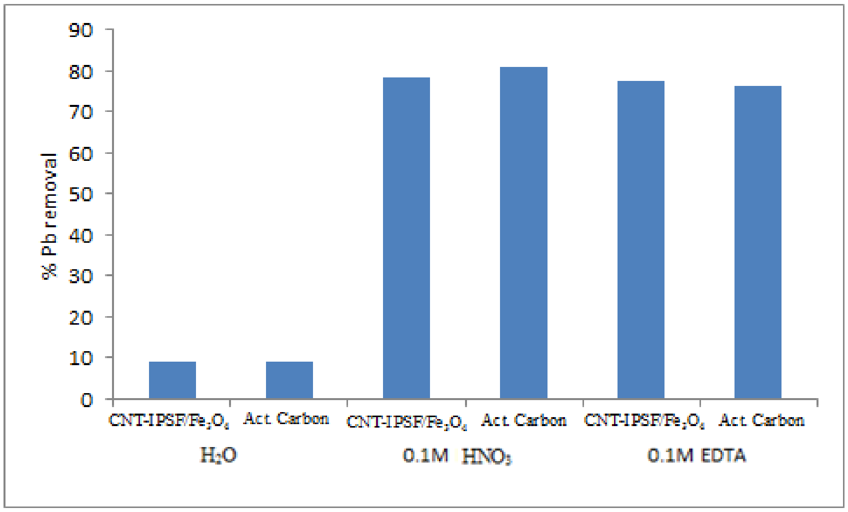

Fig. 9 Efficiencies of Pb(II) ions from CNT-IPSF/Fe_3O_4 and activated carbon

Conclusions

This paper presented a novel fabricated CNT-PSF nanocomposites for purification of contaminated water. Desired properties of the nanocomposites were confirmed from techniques such as SEM (morphology), TEM (surface distribution of nanoparticles), XRD (for crystallinity), EDS (composition), FT-IR (functional groups) and SQUID (magnetic responsiveness). The main contribution of this work is the proposed application of the nanocomposite in waste water purification. The Freundlich and Langmuir isotherm derived from the equilibrium data leverages interdisciplinary techniques including the adsorption, desorption and regeneration tests to ascertain the efficiency of the product. Studies on desorption efficiencies gave values above 60 % after three desorption cycles confirming the reusability of the fabricated magneto-responsive CNT-IPSF/Fe_3O_4 nanocomposites. The results from SQUID further confirmed that the CNT-IPSF/Fe_3O_4 nanocomposites had magneto-responsive property. The resulting new knowledge from this study has the potential to transition the current small scale purification model to an automated model, that can simultaneously improve water purification techniques and efficiency on large scale settings. From the results obtained, this process should be scaled up by dispersing the nanocomposites on contaminated water surfaces in inaccessible areas for water remediation.

References

Banerjee, S., Hemraj-Benny, T. and Wong, S. S. (2005). Covalent surface chemistry of single-walled carbon nanotubes. *Advanced Materials* 17(1): 17-29.

Díez-Pascual, A. M. (2021). Chemical functionalization of carbon nanotubes with polymers: a brief overview. *Macromol*, *1*(2), 64-83.

Han, Z. and Fina, A. (2011). Thermal conductivity of carbon nanotubes and their polymer nanocomposites: a review. *Progress in Polymer Science* 36(7): 914-944.

Kulkarni, S. A., Sawadh, P. and Palei, P. K. (2014). Synthesis and Characterization of Superparamagnetic $Fe_3O_4.SiO_2$ Nanoparticles. *Journal of Korean Chemical Society* 58.

Mallick, P. K. (2007). Fiber-reinforced composites: materials, manufacturing, and design. CRC press.

Shaaban, E., Ahmad, M., Wahab, E. A., Hassan, H. S. and Aboraia, A. (2013).Structural and optical properties of varies thickness of ZnTe nanoparticle. In *Book of Proceedings*.

Sodipo, B. K. and Aziz, A. A. (2013).Sonochemical synthesis of silica coated super paramagnetic iron oxide nanoparticles. In *Materials Science Forum*, Vol. 756, 74-79: Trans Tech Publications, Switzerland.

Spitalsky, Z., Tasis, D., Papagelis, K. and Galiotis, C. (2010). Carbon nanotube–polymer composites: chemistry, processing, mechanical and electrical properties. *Progress in Polymer Science* 35(3): 357-401.

Sun, C., Li, H. and Chen, L. (2012). Nanostructured ceria-based materials: synthesis, properties, and applications. *Energy and Environmental Science* 5(9): 8475-8505.

Wei, X., Wang, Z., Wang, J. and Wang, S. (2012). A novel method of surface modification to polysulfone ultrafiltration membrane by preadsorption of citric acid or sodium bisulfite. *Membrane Water Treatment* 3: 35-49.

Yang, S., Liu, H. and Zhang, Z. (2008). A facile route to hollow superparamagnetic magnetite/polystyrene nanocomposite microspheres via inverse miniemulsion polymerization. *Journal of Polymer Science Part A: Polymer Chemistry* 46(12): 3900-3910.

Yin, J., & Deng, B. (2015). Polymer-matrix nanocomposite membranes for water treatment. *Journal of membrane science*, *479*, 256-275.

Zheng, J.-C., Feng, H.-M., Lam, M. H.-W., Lam, P. K.-S., Ding, Y.-W. and Yu, H.-Q. (2009). Removal of Cu (II) in aqueous media by biosorption using water hyacinth roots as a biosorbent material. *Journal of Hazardous Materials* 171(1): 780-785.